Diffraction in chirped volume Bragg gratings

Jiansheng Feng (封建胜)[1,2], Xiang Zhang (张 翔)[1,2], Dengsheng Wu (吴登生)[3], Shang Wu (吴 尚)[1,2], and Xiao Yuan (袁 孝)[1,2*]

[1]College of Physics, Optoelectronics and Energy & Collaborative Innovation Center of Suzhou Nano Science and Technology, Soochow University, Suzhou 215006, China

[2]Key Lab of Advanced Optical Manufacturing Technologies of Jiangsu Province & Key Lab of Modern Optical Technologies of Education Ministry of China, Soochow University, Suzhou 215006, China

[3]Research Center of Laser Fusion, China Academy of Engineering Physics, Mianyang 621900, China

[*]Corresponding author: xyuan@suda.edu.cn

Received June 20, 2014; accepted July 16, 2014; posted online January 26, 2015

We use fundamental matrix (*F*-matrix) method derived from coupled wave theory to simplify the diffraction simulation of chirped volume Bragg grating (CVBG) and it can be applied to arbitrary grating phase profiles. With the *F*-matrix method, we study the diffraction in CVBG. The spectral response of CVBG is a gate-like function, and the passband width of spectral response is related to the product of grating thickness and spatial chirp rate. The peak diffraction efficiency of CVBG increases monotonously as the amplitude of refractive index modulation increases. Incident beams with different wavelengths will be mainly diffracted at different depths of CVBG to match the Bragg condition.

OCIS codes: 090.7330, 050.1590, 050.1940.
doi: 10.3788/COL201513.S10901.

Chirped pulse amplification (CPA) has been widely applied in lasers to obtain ultrashort laser pulse with high peak power[1,2]. The indispensable devices in CPA systems are dispersion elements such as diffraction gratings, prism pairs and fibers[3], which are used as stretchers and compressors. The most widely used dispersion element is the surface grating because of its high dispersion. However, the laser damage threshold for surface grating is still a problem and may be the limit for obtaining high-power ultrashort laser pulses. The method for increasing laser output power requires a grating of large dimensions. In petawatt-level lasers, surface gratings with ruled areas of about 1×1 (m) should be employed to obtain high-power output and avoid damage[4]. Such a huge aperture requires extreme fabrication. The chirped volume Bragg grating (CVBG), a kind of VBG of which the grating periods vary with depth, may be an alternative element as the stretcher or compressor in CPA system because of its high dispersion, high damage threshold, simple configuration, easy alignment, etc.

The first application of CVBG in CPA system was reported by Galvanauskas in 1998. With a 200 μm×300 μm ×5 mm CVBG written in hydrogen-loaded germanosilicate glass, a pulse of 500 nJ was obtained[5]. Thereafter, a series of experimental investigations on CPA systems with CVBGs recorded in PTR glass were studied[6,7]. However, the analytical theory for CVBGs[8] to the best of our knowledge is derived from Shapiro's theory[9] and is applied only for quasi-sinusoidal grating with quadratic phase. The finite difference time domain (FDTD) method, in which the mesh size is about $\lambda/10$ (where λ is the interested wavelength), requires large amount of calculation. Even though the transfer matrix method requires the mesh size smaller than Λ/N (where Λ is the grating period), it still requires much calculation capacity. However, the fundamental matrix (*F*-matrix) method proposed in this letter requires mesh size of more than Λ, and simulation can be realized in personal computer.

F-matrix method can also be applied to arbitrary grating phase profiles. In this method, the CVBG is divided into multiple uniform-period VBGs, and each grating is characterized with a *F*-matrix[10] which can be derived from the classical coupled wave theory[11]. With the method, the diffraction in CVBG is studied. The spectral response of CVBG is a gate-like function, and the passband width is related to the product of grating thickness and spatial chirp rate. The broad spectral response of CVBG is due to the beams whose different wavelengths are diffracted at different depths of CVBG.

The uniform-period VBG owns cosinoidal refractive index and a uniform grating period, and the wave equation for uniform-period VBG is a Mathieu's differential equation. Based on the analytical solutions of this equation, the coupled wave theory[11] and the rigorous coupled wave theory[12] can be used to characterize the VBG. The CVBG, however, has the grating period varying along the depth. The wave equation for the CVBG is more complex, and the solution to this equation is far more different from that of the Mathieu function. So the coupled wave theory or rigorous coupled wave theory cannot be directly used to characterize CVBGs. While considering a small part of

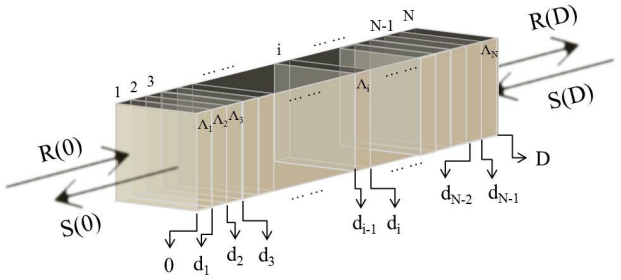

Fig. 1. Uniform decomposition of CVBG.

a CVBG, the variation of grating period can be negligible and thus such a small part can be treated as an individual uniform-period VBG. Thus, the whole CVBG can be regarded as the congregation of the uniform-period VBGs. The CVBG discussed in this letter is an unslanted reflective one with linear chirping, and operates at normal incidence. The refractive index of CVBG is

$$n(z) = n + \Delta n \cos(\varphi(z)), \tag{1}$$

where n is the average refractive index, Δn ($\Delta n \ll n$) is the amplitude of refractive index modulation, $\varphi(z)$ is the grating phase, with which the grating period and spatial chirp rate can be derived. For a VBG, the grating phase is linear with respect to depth. For a linear chirped CVBG, however, it is a logarithmic function. The refractive index outside the CVBG is assumed to be the same as the average refractive index n.

As shown in Fig. 1, a CVBG is divided into N uniform-grating VBGs which are small enough to be regarded as uniform-period VBGs, and these VBGs have their own parameters such as grating thicknesses and grating periods. The VBG is well studied with the classical coupled wave theory, and we rewrite this theory to obtain more common results with which the adjacent VBGs can be mathematically connected effectively. Only two waves are assumed to propagate in VBGs as usual, the reference wave R and the signal wave S, and the coupled wave equations[11] are obtained.

$$\begin{cases} \dfrac{\mathrm{d}R}{\mathrm{d}z} = -i\kappa S - \alpha R \\ \left(1 - \dfrac{\lambda}{2n\pi}\right)\dfrac{\mathrm{d}S}{\mathrm{d}z} = -i\kappa R - (\alpha + i\vartheta)S \end{cases}, \tag{2}$$

where R and S are the complex amplitudes of the reference beam and signal beam, $\vartheta = 2\pi/\Lambda - \pi\lambda/n\Lambda$ is the dephasing parameter, $\kappa = \pi\Delta n/\lambda - j\alpha_1/2$ is the coupling constant, λ is the incident wavelength in free space, Λ is the grating period of the VBG, α is the average absorption constant, and α_1 is the absorption constant modulation.

The general solution of Eq. (2) is

$$\begin{cases} R(z) = r_1 \exp(\gamma_1 z) + r_2 \exp(\gamma_2 z) \\ S(z) = s_1 \exp(\gamma_1 z) + s_2 \exp(\gamma_2 z) \end{cases}. \tag{3}$$

We insert Eq. (3) into the coupled wave Eq. (2), and compare the terms with equal exponentials ($\exp(\gamma_1 z)$ and $\exp(\gamma_2 z)$). Then the constants γ_1 and γ_2 are obtained.

$$\gamma_{1,2} = -\frac{1}{2}\left(\alpha + \frac{\alpha}{1-\lambda/2n\Lambda} + i\frac{\vartheta}{1-\lambda/2n\Lambda}\right) \pm \frac{1}{2}\left[\left(\alpha - \frac{\alpha}{1-\lambda/2n\Lambda} - i\frac{\vartheta}{1-\lambda/2n\Lambda}\right)^2 - 4\frac{\kappa^2}{1-\lambda/2n\Lambda}\right]^{1/2} \tag{4}$$

And with the expression of γ_i (i = 1, 2), the coefficients r_i and s_i (i = 1, 2) can be obtained. They are interrelated as

$$\begin{cases} s_1 = \dfrac{\gamma_1 + \alpha}{-i\kappa} r_1 \\ s_2 = \dfrac{\gamma_2 + \alpha}{-i\kappa} r_2 \end{cases}. \tag{5}$$

In general, once the boundary conditions are established, r_i and s_i (i = 1, 2) can be simply derived. In order to get a more general formalism about the reference wave and signal wave, the ith VBG ($d_{i-1} \le z \le d_i$) is written as

$$\begin{bmatrix} R(d_{i-1}) \\ S(d_{i-1}) \end{bmatrix} = F_i \begin{bmatrix} R(d_i) \\ S(d_i) \end{bmatrix} = \begin{bmatrix} F_{11}^{(i)} & F_{12}^{(i)} \\ F_{21}^{(i)} & F_{22}^{(i)} \end{bmatrix} \begin{bmatrix} R(d_i) \\ S(d_i) \end{bmatrix}, \tag{6}$$

where F_i is the F-matrix of the ith VBG, and this formalism can simplify the congregation of N individual uniform-period VBGs.

Combining Eqs. (3) and (6), and comparing the terms with equal constants (r_1 and r_2), the matrix F_i can be obtained as

$$F_{11}^{(i)} = \frac{-(\gamma_2^{(i)} + \alpha^{(i)})\exp(-\gamma_1^{(i)} d^{(i)})}{\gamma_1^{(i)} - \gamma_2^{(i)}} + \frac{(\gamma_1^{(i)} + \alpha^{(i)})\exp(-\gamma_2^{(i)} d^{(i)})}{\gamma_1^{(i)} - \gamma_2^{(i)}}, \tag{7}$$

$$F_{12}^{(i)} = -i\kappa^{(i)} \cdot \frac{\exp(-\gamma_1^{(i)} d^{(i)}) - \exp(-\gamma_2^{(i)} d^{(i)})}{\gamma_1^{(i)} - \gamma_2^{(i)}}, \tag{8}$$

$$F_{21}^{(i)} = (\gamma_1^{(i)} + \alpha^{(i)})(\gamma_2^{(i)} + \alpha^{(i)}) \cdot \frac{\exp(-\gamma_1^{(i)} d^{(i)}) - \exp(-\gamma_2^{(i)} d^{(i)})}{i\kappa^{(i)} \cdot (\gamma_1^{(i)} - \gamma_2^{(i)})}, \tag{9}$$

$$F_{22}^{(i)} = \frac{(\gamma_1^{(i)} + \alpha^{(i)})\exp(-\gamma_1^{(i)} d^{(i)})}{\gamma_1^{(i)} - \gamma_2^{(i)}} - \frac{(\gamma_2^{(i)} + \alpha^{(i)})\exp(-\gamma_2^{(i)} d^{(i)})}{\gamma_1^{(i)} - \gamma_2^{(i)}}, \tag{10}$$

where $d^{(i)} = d_i - d_{i-1}$ is the thickness of the ith VBG.

According to Eq. (6), the F-matrix of a CVBG is the product of F-matrices of the N uniform-period VBGs

$$\overline{F} = \begin{bmatrix} \overline{F}_{11} & \overline{F}_{12} \\ \overline{F}_{21} & \overline{F}_{22} \end{bmatrix} = F_1 F_2 \cdots F_i \cdots F_N. \tag{11}$$

With the boundary conditions $R(0)=1$ and $S(d)=0$, the complex amplitude of the signal wave diffracted by the CVBG is $S(0) = \overline{F}_{21}/\overline{F}_{11}$, and the diffraction efficiency is

$$\eta = \overline{F}_{21}\overline{F}_{21}^{*}/\overline{F}_{11}\overline{F}_{11}^{*}. \tag{12}$$

The division of a CVBG is arbitrary, but has to keep the continuity of CVBG. In other words, the grating phase at the interface between two adjacent VBGs must satisfy continuity condition, which is described as

$$\varphi_k = \varphi_{k-1} + 2\pi d_{k-1}/\Lambda_{k-1}, \tag{13}$$

where $\varphi_{k-1}+2\pi d_{k-1}/\Lambda_{k-1}$ represents the grating phase at the end of the $(k-1)$th VBG and φ_k is the early grating phase of kth one.

The diffraction properties of CVBG are discussed with F-matrix method. The curve in Fig. 2(a) represents the gate-like spectral response of CVBG with central grating period of 343 nm, spatial chirp rate of 3 nm/cm, thickness of 1 cm, and the amplitude of refractive index modulation of about 600 ppm. The passband width of spectral response of CVBG is about 9 nm (full-width at half-maximum, FWHM). The inset of Fig. 2(a) shows the comparison between the F-matrix method and the transform matrix method. The simulation results obtained from these two methods match well.

In F-matrix method, the CVBG is the congregation of VBGs with different grating periods and Bragg wavelengths. Since the diffraction takes place only when the wavelength of incident beam equals the Bragg wavelength of VBG, beams with wavelengths outside the passband of CVBG will simply pass through and only the ones with wavelengths inside the passband will be efficiently diffracted and reflected back. Apart from VBG, CVBG owns a wider passband which can be up to 100 nm, and the passband width is determined by the product of thickness and spatial chirp rate as

$$\Delta B = 2n \cdot D \cdot (\mathrm{d}\Lambda/\mathrm{d}z), \tag{14}$$

where D is the thickness of CVBG, $(\mathrm{d}\Lambda/\mathrm{d}z)$ is the spatial chirp rate, and the average refractive index $n = 1.5$.

The curve of diffraction efficiency at the passband from 1025.5 to 1034.5 nm is almost flat. Some oscillations exist around 73%, which is the diffraction efficiency at the central wavelength 1030 nm and chosen as the peak diffraction efficiency of CVBG for simple. Higher peak diffraction efficiency can be obtained by increasing the amplitude of refractive index modulation (Fig. 2(b)). When the amplitude of refractive index modulation and grating thickness are fixed values, diffraction efficiency can also be improved by decreasing the spatial chirp rate. This improvement, however, will result in decreasing of passband width as shown in Eq. (14).

As shown in Fig. 3(a), the CVBG is divided into 15 parts with same thickness. The diffraction efficiency curve of each part takes the same shape due to the same amplitude and form of refractive index modulation. The passband width of each part is about 0.7 nm (FWHM), which is a little wider than 1/15 of the passband width of CVBG due to spectral overlapping.

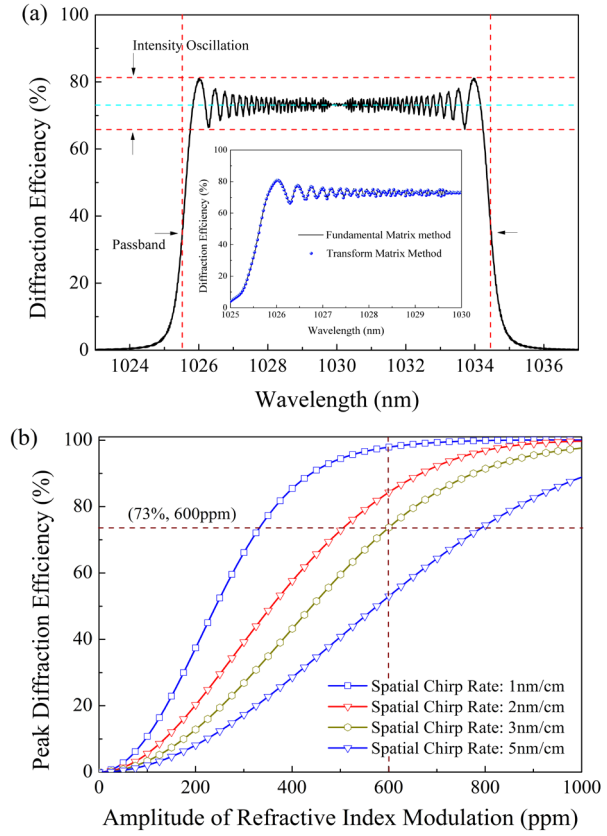

Fig. 2. (a) Spectral response of CVBG and (b) peak diffraction efficiency versus refractive index modulation and spatial chirp rate.

The incident beams with different wavelengths are diffracted at different depths of CVBG. As shown in Fig. 3(b), the diffraction efficiency peaks at the center of each part and corresponds to a certain wavelength between 1025.5 and 1034.5 nm, varying along the grating depth. An incident beam with the wavelength of 1028.2 nm will be mainly diffracted by the No. 5 part of which the diffraction efficiency at 1028.2 nm is of 69%, while the adjacent parts (Nos. 4 and 6) shows low diffraction efficiencies at 1028.2 nm, and the diffraction efficiencies of parts far away from No. 5 are much lower. Thus, most of incident beam power is diffracted by the main part (such as the No. 5 part for beam with wavelength of 1028.2 nm), and coherent superposition of diffraction by the parts before and after the main one results in diffraction efficiency oscillation.

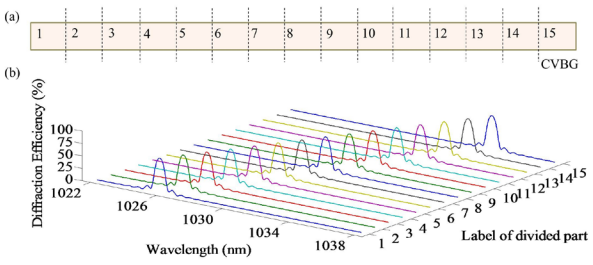

Fig. 3. (a) Division of CVBG and (b) diffraction in CVBG.

The *F*-matrix method is discussed to simplify the diffraction simulation of CVBG. CVBG is divided into multiple uniform-period VBGs, and each VBG is characterized with an *F*-matrix derived from the classical coupled wave theory. Then, the *F*-matrices of all VBGs are multiplied together. A new *F*-matrix is obtained, from which the diffraction efficiency of CVBG can be obtained. The basic mesh of *F*-matrix method is VBG, and it needs less calculation amount than the transfer matrix method or FDTD. With the *F*-matrix method, simulation of CVBG of thickness of more than tens of centimeters can be done in personal computer.

In conclusion, we study diffraction in CVBG. The passband width of spectral response of CVBG is related to the product of thickness and spatial chirp rate. As the amplitude of refractive index modulation increases, peak diffraction efficiency of CVBG increases monotonously. With a fixed grating thickness, decreasing the spatial chirp rate can also improve the peak diffraction efficiency. Although incident beam with a certain wavelength will mostly be diffracted at a corresponding depth of CVBG to match the Bragg condition, coherent superposition of diffraction by other parts of CVBG will increase or decrease the efficiency and lead to diffraction efficiency oscillation of CVBG.

This work was supported by the National Natural Science Foundation of China (NSFC; Nos. 91023009 and 61275140), the United Foundation of NSFC and the Chinese Academy of Engineering Physics (Nos. 11176021 and 11076021), the Natural Science Foundation of Jiangsu Higher Education Institutions (No. 10KJA140045), a Project Funded by the Priority Academic Program Development of Jiangsu Higher Education Institutions, the National 863 Program of China, and the Graduate Research and Innovation Project of Jiangsu Province (Nos. CXZZ12_0813 and CXZZ13_0808).

References

1. D. Strickland and G. Mourou, Opt. Commun. **56,** 219 (1985).
2. M. Hemmer, A. Thai, M. Baudisch, H. Ishizuki. T. Taira, and J. Biegert, Chin. Opt. Lett. **11,** 013202 (2013).
3. C. Zhang, X. Wang, W. Fan, D. Rao, and Z. Lin, Chin. Opt. Lett. **11,** 070606 (2013).
4. M. D. Perry and G. Mourou, Science **264,** 917 (1994).
5. A. Galvanauskas, A. Heaney, T. Erdogan, and D. Harter, in *Proceedings of CLEO* CThJ2 (1998).
6. K. H. Liao, C. H. Liu, G. Almantas, F. Emilie, I. S. Vadim, and B. G. Leonid, in *Proceedings of Advanced Solid-State Photonics* 768 (2005).
7. C. P. Joao, H. Pires, L. Cardoso, T. Imran, and G. Figueira, Opt. Express **22,** 10097 (2014).
8. S. Kaim, S. Mokhov, B. Y. Zeldovich, and L. B. Glebov, Opt. Eng. **53,** 051509 (2013).
9. O. V. Belai, E. V. Podivilov, and D. A. Shapiro, Opt. Commun. **266,** 512 (2006).
10. M. Yamada and K. Sakuda, Appl. Opt. **26,** 3474 (1987).
11. H. Kogelnik, Bell Syst. Tech. J. **48,** 2909 (1969).
12. M. G. Moharam and T. K. Gaylord, J. Opt. Soc. Am. **71,** 811 (1987).